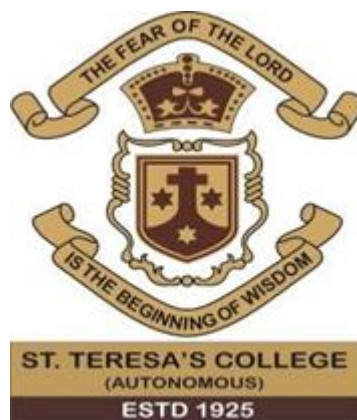


PROJECT REPORT
ON
**PHOTOLUMINESCENCE PROPERTY OF NICKEL
FERRITE NANOPARTICLES**

SUBMITTED BY
MERLIN C BIJU
REGISTER NO.: AM21PHY012

in partial fulfillment of
the requirements for award of the postgraduate degree in physics



**DEPARTMENT OF PHYSICS AND CENTRE FOR RESEARCH
ST.TERESA'S COLLEGE (AUTONOMOUS) ERNAKULAM
2021-2023**

ST TERESA'S COLLEGE (AUTONOMOUS) ERNAKULAM



M.Sc. PHYSICS PROJECT REPORT

Name : MERLIN C BIJU

Register Number : AM21PHY012

Year of Work : 2021-23

This is to certify that the project "PHOTOLUMINESCENCE PROPERTY OF NICKEL FERRITE NANOPARTICLES" is the work done by MERLIN C BIJU.

Dr. Priya Parvathi Ameen Jose

Head of the Department



Dr. Mariyam Thomas

Guide in charge

Submitted for the University Examination held at St. Teresa's College, Ernakulam

Date : 7-6-2023

Examiners 1) Dr. REKHA S. Rekha S. 7/6/23

2) Dr. Louie Frobela P. G. Louie P. G. 7/6/23


DEPARTMENT OF PHYSICS

ST TERESAS COLLEGE (AUTONOMOUS), ERNAKULAM

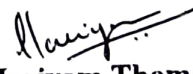


CERTIFICATE

This is to certify that the project report entitled “**PHOTOLUMINESCENCE PROPERTY OF NICKEL FERRITE NANOPARTICLES**” is the Bonafide work done by **Ms. MERLIN C BIJU** (Reg. No: AM21PHY012) under the guidance of **Dr. MARIYAM THOMAS**, Assistant Professor, Department of Physics and Centre for Research, St. Teresa’s College, Ernakulam in partial fulfilment of the award of the Degree of Master of Science in Physics, St. Teresa’s College, Ernakulam affiliated to Mahatma Gandhi University, Kottayam


Dr. Priya Parvathi Ameena Jose
Head of the Department




Dr. Mariyam Thomas
Guide in charge

DECLARATION

I, hereby declare that the project work entitled "**PHOTOLUMINESCENCE PROPERTY OF NICKEL FERRITE NANOPARTICLES**" is a record of an original work done by me under the guidance of **Dr .MARIYAM THOMAS**, Assistant Professor, Department of Physics and Centre for Research, St Teresa's College, Ernakulam in the partial fulfilment of the requirements for the award of the Degree of Master of Physics. I further declare that the data included in the project is collected from various sources and are true to the best of my knowledge.


MERLIN C BIJU

ST.TERESA'S COLLEGE (AUTONOMOUS) ERNAKULAM

Certificate of Plagiarism Check for Thesis

Author Name	Merlin C Biju
Course of Study	MSc Physics
Name of Guide	Dr. Mariyam Thomas
Department	Physics & Centre For Research
Acceptable Maximum Limit	20%
Submitted By	library@teresas.ac.in
Paper Title	PHOTOLUMINESCENCE PROPERTY OF NICKEL FERRITE NANOPARTICLES
Similarity	2%
Paper ID	758764
Submission Date	2023-06-01 12:42:16

Signature of Student

Signature of Guide

Checked By
College Librarian*** This report has been generated by DrillBit Anti-Plagiarism Software**

ACKNOWLEDGEMENT

The success and final outcome of this project required a lot of guidance and assistance from many people and we are extremely grateful to have got this all along the completion of my project work. Primarily, we thank God almighty for being with us throughout all the days and helping us complete the project successfully.

It is with great pleasure I express my sincere gratitude to Dr. Mariyam Thomas, my supervising guide, for his able guidance and encouragement throughout the course of this work and I am deeply indebted for the personal support you had given me during moments of uncertainty.

I would like to thank Dr. Priya Parvathi Ameena Jose, Head of the Department of Physics, St. Teresa's (Autonomous) College, Ernakulam for her support and guidance.

I also express my sincere thanks to Aneena Elizabeth George for her whole hearted cooperation and help. A special thanks to my family for being a strong pillar in times of stress and struggle.

CONTENTS

Abstract.....	9
---------------	---

CHAPTER 1

1.Introduction.....	10
1.1 Ferrites.....	10
1.2 Structure of Nickel Ferrite.....	14
1.3 Properties of Nickel Ferrite.....	15
1.4 Applications of Nickel Ferrite.....	15
1.5 Photoluminescence.....	15
1.6 Applications of Photoluminescence	18

CHAPTER 2

2.Experimental Techniques.....	20
2.1 Solgel method.....	20
2.2 Coprecipitation method.....	22
2.3 x-ray diffraction.....	23
2.4 Scanning electron microscopy (SEM).....	26
2.5 UV-visible spectroscopy.....	29
2.6 Photoluminescence.....	30

CHAPTER 3

3.Results and Discussions.....	23
3.1 Structural Characterization.....	23
3.2 Morphological Analysis'.....	39
3.3 Optical Characterization.....	40
3.4 Conclusions.....	45
3.5 Future Scope.....	45
3.6 References.....	46

ABSTRACT

Sol gel and co-precipitation technique have been used to synthesize Nickel Ferrite ($NiFe_2O_4$) nanoparticles. In both the methods, the samples were calcinated for 2 hrs at $400^{\circ}C$ and structural, morphological and optical properties of nickel ferrite were investigated. XRD (X-ray diffraction) were used to examine the structural properties and it reveals a spinal cubic structure. SEM (Scanning Electron Microscope) gives the morphological details and it confirms highly crystallized agglomerated irregular morphology. Optical properties were studied by uv-visible absorption spectroscopy and photoluminescence spectroscopy.

This project is an attempt to understand the photoluminescence behaviour of Nickel Ferrite ($NiFe_2O_4$) nanoparticles.

CHAPTER 1

INTRODUCTION

1.1 FERRITES

Ferrites are a class of magnetic oxides that contain iron oxides as their main constituent. They are ceramic materials and exhibit ferrimagnetic behavior. Ferrites are polycrystalline, which means they are made up of a lot of microscopic crystals and are hard, brittle, iron-containing, and typically black or grey. These are chemically made up of iron oxide as well as additional metals. Ferrimagnetism is a form of magnetism is seen in solids. Typically, ferrites are ceramic compounds with ferrimagnetic properties that are formed from iron oxides. Magnetite (Fe_3O_4) is used as a well-known illustration. Similar to the majority of various ceramics, ferrites are hard, brittle, and poor electrical conductors. Many ferrites have the spinel structure, which has the formula AB_2O_4 , in which A and B represent metal cations, typically including iron. The typical structure of spinel ferrites is cubic close-packed (fcc), one by eight of tetrahedral voids are occupied by A cations and octahedral holes are occupied by B cations. They are of formulae $\text{A}^{2+}\text{B}_2^{3+}\text{O}_4^{2-}$

Based on magnetic properties, Ferrites are classified into Soft Ferrites and Hard Ferrites.

SOFT FERRITES

Ferrite crystals have inverse spinel structure rather than the common spinel structure: The B cations occupy one-eighth of the tetrahedral holes and one fourth of octahedral sites. Cations occupy one fourth of octahedral sites. Zinc, nickel, and manganese-containing compounds are present in ferrites, which are employed as a transformer core material. They are referred to as soft ferrites and have a low coercivity. High resistivity of the material avoids eddy currents in the core also energy source losses, but low coercivity reverses the direction of

magnetization without consuming additional energy (hysteresis losses). They can be widely utilised in radio frequency transformers as well as cores of inductor. applications include switched-mode power supplies antennas and loop stick utilized in AM radios due to their relatively low losses at higher frequencies.

HARD FERRITES

In contrast, the permanent ferrite magnets are made of hard ferrites that contain a high remanence and high coercivity after magnetization. Barium and iron oxide or strontium carbonate can be used in the manufacturing of hard ferrite magnets. High coercivity is defined as the materials that are more resistant to becoming demagnetized, an important characteristic for a permanent magnet. Also, they hold a high magnetic permeability. These are in particular called ceramic magnets are very cheap and widely used in the household products like refrigerator magnets. after magnetization hard ferrites which exhibit high coercivity as well as high remanence are used to make permanent ferrite magnets. Hard ferrite magnets can be made using barium or strontium carbonate. High coercivity is characterised by the materials increased resistance to demagnetization, which is a crucial quality for a permanent magnet. They possess a strong magnetic permeability as well. These specific ceramic magnets are incredibly affordable and frequently used in home items like refrigerator magnets.

Based on crystal structure, Ferrites are classified into

SPINEL FERRITES

A Spinel ferrite is a ferrimagnetic material, represented by the formula MFe_2O_4 . M is a divalent metal ion like cobalt, nickel, copper, manganese, magnesium, zinc, cadmium etc. The structure of spinel ferrite is a close packed cubic structure of oxygen atoms with eight formula units per unit cell.

The radius of oxygen ion is of the order of 1.32Å which is much greater than the metal ions, which is in the range of 0.6 to 0.8Å, hence the oxygen ions in this lattice touch each other and form a close packed face centred cubic lattice.

The unit cell of spinel ferrite consists of two sub lattices namely tetrahedral [A] and octahedral [B] sites. Tetrahedral site is smaller than octahedral site.

Tetrahedral site and octahedral site can both accommodate a variety of cations, allowing for substantial variation in the characteristics of ferrites. M can be substituted with various divalent metal ions to produce a variety of spinel ferrites. An fcc cubic close packed structure of oxygen anions with one-eighth filled tetrahedral (A) sites and one-half filled octahedral (B) sites makes up the ideal spinel structure. Eight AB_2O_4 formula units make up one unit cell, which has 16 octahedral sites and 64 tetrahedral sites. Spinel ferrite has the chemical formula MFe_2O_4 in which M is a divalent metal ion.

GARNET FERRITES

Ferrimagnetic garnet has the chemical formula $Me_3Fe_5O_{12}$, where Me represents a trivalent ion like yttrium or a rare earth. The cubic unit cell has eight molecules of $Me_3Fe_5O_{12}$, or 160 atoms. Three different types of locations are where the metal ions are dispersed. Eight oxygen ions surround the Me ions in the dodecahedral sites also known as c sites, while the Fe^{3+} ions are dispersed among the octahedral as well as tetrahedral sites in a 2:3 ratio.

ORTHO FERRITES

The usual formula for ortho-ferrites is $MeFeO_3$, where Me is a massive trivalent metal ion, like a rare-earth ion or Y. Most orthoferrites are mildly ferromagnetic and possess an orthorhombic crystal form. The iron ion subsystem organises into a somewhat canted antiferromagnetic structure exhibiting antiferromagnetic moment G and a mild ferromagnetic moment F at the Neel temperature T_N . By interacting with the iron subsystem, this rare earth ion subsystem gains

magnetization m . Due to their antisymmetric exchange interaction that uses cross product of neighbouring spins rather than the more common scalar product, orthoferrites are particularly intriguing. The orthoferrites would have been antiferromagnetic without this interaction.

HEXAGONAL FERRITES

Numerous ferrites can form hexagonal crystals, and a few of these have recently attained significant technological significance. They are further split into the compounds M, W, Y, Z, and U. All of these have unique crystal structures that are yet connected. The structure of the M compounds is the least complex. This class includes the well-known hard ferrites barium ferrite. These substances have the fundamental formula. Me represents divalent ion with a high ionic radius, and formulae $\text{MeFe}_{12}\text{O}_{19}$.

PROPERTIES OF FERRITES

High electrical resistivity, low eddy current and dielectric losses, high saturation magnetization, high permeability, moderate permittivity, spontaneous magnetization, and conductivity behaviour are only a few of the important characteristics of ferrites. Ferrites have high saturation magnetization compared to diamagnets or paramagnets, but as they are ferrimagnets, they have much lower saturation magnetization than ferromagnets. saturation magnetization is therefore not as high as it is for other materials that are also thought to be magnetic materials. The permeability is also not that high. Ferrites display ferrimagnetism, a sort of permanent magnetism. Neel first suggested ferrimagnetism to explain the magnetic order in ferrites. In ferrimagnetism, atoms magnetic moments line up in parallel and antiparallel directions, just like in ferromagnetism and anti-ferromagnetism, respectively. Due to a partial cancellation of the magnetic field, the overall strength of the magnetic field in ferrite is smaller than that of ferromagnetic materials. Like ferromagnetic materials, ferrimagnetic materials

show a magnetic moment even in the absence of a magnetic field (spontaneous magnetic moment) below the Curie temperature. Ferrimagnetic materials also show paramagnetic behaviour above curie temperature similar to ferromagnetic materials.

1.2 STRUCTURE OF NICKEL FERRITE

Nickel Ferrite is considered as a major material of interest due to its various properties and wide level of applications. Structure of Nickel Ferrite is inverse spinel structure. It has the general formulae $B(AB)O_4$ where the divalent ion is [A] and trivalent ion is [B]. The octahedral sites are occupied by Ni^{2+} ions. The Fe^{3+} ions occupy both the tetrahedral and octahedral sites equally. The crystal structure is completed by adding oxygen atoms.

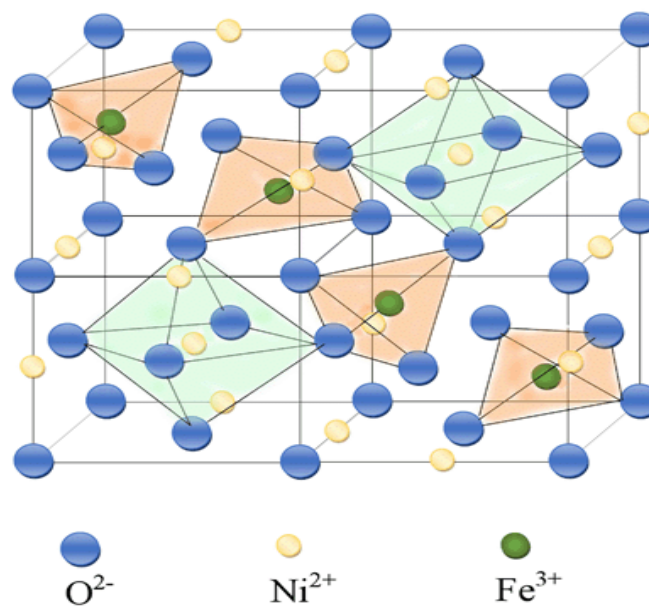


Figure 1; structure of nickel ferrite

1.3 PROPERTIES OF NICKEL FERRITE

Nickel Ferrite, which is an indirect band gap material, also abundant in nature is chemically stable and are less toxic. It is a soft ferromagnetic material with moderate coercivity and high permeability. Conductivity is small and eddy current losses are also small. Nickel Ferrite find uses in magnetic resonance

imaging, photomagnetic materials, gas sensors etc. It is also used in site specific drug delivery and as a catalyst. The nickel ferrites have excellent resistivity, retentivity, optimal saturation magnetization, and extremely high stability. Due to its typical ferrimagnetic characteristics, nickel ferrite is one of the versatile and technologically significant soft ferrite materials.

1.4 APPLICATIONS OF NICKEL FERRITE

Nickel Ferrite has a wide range of uses, including as a gas sensor, magnetic fluid, catalyst, magnetic storage system, photomagnetic material, site-specific drug delivery system, magnetic resonance imaging system, and microwave devices. Also has uses in water purification, electronic gadgets, electromagnetic wave absorption materials, and medical therapy.

1.5 PHOTOLUMINESCENCE

Luminescence is an important property of Nickel Ferrite. When a material absorbs light from sources such as UV rays or X ray's electrons are excited from lower level to a higher level. Since the excited levels are unstable the electrons return to the ground state with the emission of light. Electromagnetic radiation causes photoluminescence, which can vary from visible light through ultraviolet and X-ray. It has been established that the wavelength of the light that is emitted in photoluminescence is greater than or equal to the wavelength of the light that stimulates it. This difference in wavelength is due to the atoms or ions non-radiative vibrational energy.

Fluorescence, phosphorescence, and chemiluminescence are the three main types of luminescence in use. Two types of photoluminescence are fluorescence and phosphorescence. In photoluminescence, a material glows in response to light whereas in chemiluminescence, a chemical reaction results in the glow. The basis for each fluorescence and phosphorescence is a substance's capacity to absorb light and then produce light with a longer wavelength and, consequently, lesser

energy. The duration of time involved is the primary distinction. Phosphorescent material may store the absorbed light for a period of time and emit light later. This results in an afterglow that persists after the light is finally switched off. Fluorescent material can emit light almost instantly and is therefore typically only visible if the light source is constantly on (such as UV lights). This afterglow might linger anywhere within a few seconds to hours, depending on the material.

A radiative transition in which light is emitted from the lowest excited singlet state (S_1) to ground state (S_0) (10^{-9} to 10^{-6} sec) is known as fluorescence. It is one radiative mechanism by which excited electrons may relax. Emitting a photon allows the dissipation of the difference in energy between these layers. The radiated photon will have a lower energy and longer wavelength because the electron has lost some of the initial excitation energy through vibrational relaxation. Emission can often relax to a number of ground state vibrational levels, giving rise to a range of potential photon wavelengths. If necessary, non-radiative vibrational relaxation can help electrons move across higher vibrational levels ($v=n$) to a vibrationless state ($v=0$). Since excited molecules often decay to the lowest vibrational level of lower excited state by non-radiative mechanisms before fluorescence emission occurs, the resulting emitted wavelength will be independent of the excitation wavelength. Non-radiative decay may dissipate a smaller or larger proportion of the excitation energy depending on the molecule, causing molecule-specific changes within the excited and emitted wavelengths. This is called Stokes shift. The excitation and emission spectra of a molecule are jointly defined by the potential wavelength of a photon that could be absorbed during excitation and the potential emission wavelengths, which vary due to fluorescence decay into different vibrational levels.

We need to take a brief diversion into electron spin to explain the distinction between fluorescence and phosphorescence. The behaviour in a field of electromagnetic radiation is determined by the electron's spin, which is a type of

angular momentum. Electron spin has a maximum value of $1/2$ and can only have one of two orientations: up or down. The spin of an electron is therefore expressed as $+1$ or -1 . At the singlet ground state (S_0), a pair of electrons in the same orbital possess an antiparallel spin. A singlet excited state (S_1) is created when one electron is promoted into an excited state while still maintaining its spin orientation. In this condition, the two spin orientations continue to be paired as antiparallel. Fluorescence relaxation processes are all spin-neutral, and the electron's spin orientation is always preserved.

In contrast, phosphorescence is a separate phenomenon. The electron spin is inverted because of intersystem crossing from a singlet excited state (S_1) to an energetically advantageous triplet stimulated state (T_1). The parallel spin of two electrons in triplet excited states distinguishes them as metastable. Through phosphorescence, which causes another flipping of the electron spin plus the emission of a photon, relaxation takes place. The transition back to the singlet ground state (S_0) could take anywhere between 10^{-3} and 100 seconds. Additionally, more energy is lost through non-radiative processes while phosphorescent relaxation than during fluorescence, resulting in a larger energy gap between the photons that are absorbed and released and a more noticeable wavelength shift. The Stokes shift of phosphorescence is larger than that of fluorescence.

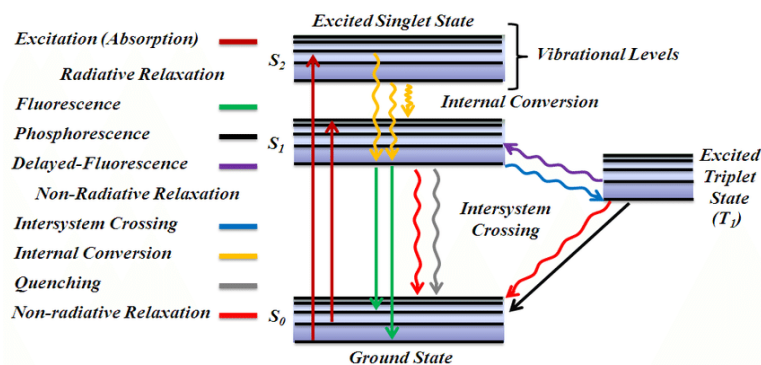


Figure 2: Jablonski diagram

1.6 APPLICATIONS OF PHOTOLUMINESCENCE

Fluorometry is a very effective technique that analyses the material's visible emission after it has been emitted, providing information on the material. It has several applications. Impurity analysis by comparing the specimen's PL spectrum to a reference spectrum. This method is frequently employed in the medical profession and tablet industry. It is also feasible to identify and evaluate many fluorescing chemicals in a single solution. Fluorometry has applications in biology and medicine as well. It provides information on vitamin deficiencies, blood, urine, and hormone concentrations. Pus, blood, and urine are employed in chromatographic separation for strain identification and toxin detection

The internal lamp wall of fluorescent lamps and compact fluorescent lamps (CFLs) is plastered with phosphors. Electric discharge produces UV light with a wavelength of 253.7 nm. UV is absorbed by phosphor and transforms it into visible light by fluorescence emission. The type of phosphor used in fluorescent lamps determines the colour of its output. There are now many different types of fluorescent bulbs on the market.

Different luminescent materials exhibit visible emission of various colours when exposed to ionising radiations. The existence of radiation field can be determined by preparing the screen with luminous material. This feature of phosphors is being applied to watch dials, television picture tubes, and other surfaces. Material's luminescent emission is extremely sensitive to the specimen's composition, structure, and impurity (or defect). if we take a PL spectrum of a specimen it is like a fingerprint of the specimen. Therefore, much information may be learned by comparing the PL pattern of an ideal specimen with that of a specimen in a different state. These facts are used in forensic science to track down criminals and prosecute them, among other things. It also assesses the specimen's Physico-chemical state. In forensic science, it can be used to identify substances When different elements in a sample are bombarded with electrons or

X-rays and release distinctive lines, the elements can be identified by examining the radiation that is emitted. By examining the intensity and distinctive characteristics of the material's emission, one can measure the coating thickness of one chemical over another. Chemical behaviour of liquids may also be examined using the fluorescence emission method. Fluorescence is frequently utilised in the analysis of different chemicals found in liver, kidney, and other cell types. Professionals can estimate amino acids, proteins, and nucleic acids in medico-legal tasks. The luminescence technique is used in numerous biological experiments to identify and quantify bacteria and viruses. Luminescence is a phenomenon that is highly sensitive to structure and is capable of detecting patterns within the materials' lattice. Examining fluorescence spectra can reveal host matrix wrong patterns.

CHAPTER 2

EXPERIMENTAL TECHNIQUES

Hydrothermal, co-precipitation, microwave, reverse micelle, solvothermal, combustion synthesis, ball milling etc. are usually used to prepare nickel ferrite nanoparticles. Due to its ease of use and the high quality and chemical purity of the nickel ferrite produced, combustion synthesis is one of the methods that is frequently employed to create nickel ferrite.

Here to prepare NiFe_2O_4 nanoparticles we used solgel and coprecipitation method.

2.1 SOLGEL METHOD

Solgel method was used to synthesize Nickel Ferrite nanoparticles at room temperature.

1. Nickel Nitrate hexahydrate $[\text{Ni}(\text{NO}_3)]_2 \cdot 6\text{H}_2\text{O}$, Iron Nitrate Nonahydrate $[\text{Fe}(\text{NO}_3)_2] \cdot 9\text{H}_2\text{O}$ and Citric acid ($\text{C}_6\text{H}_8\text{O}_7 \cdot \text{H}_2\text{O}$) are used as the starting materials.



Figure 1: Citric acid

figure 2: iron nitrate

figure 3: nickel nitrate

2. Here the ratio of metal to citric acid is taken as 1:1.

$$\text{Weight of the salt required (w)} = \frac{\text{Molarity} \times \text{Molecular mass} \times \text{Volume}}{1000}$$

Molecular Mass of Nickel Nitrate = 290.79g

Molecular Mass of Iron Nitrate = 404g

Molecular Mass of Citric Acid=210.14g

Weight of Nickel Nitrate==2.9079g

weight of Iron Nitrate==8.08g

weight of Citric acid==2.1014g

3.They are dissolved using stoichiometric amount of de-ionised water and stirring using a magnetic stirrer attached with hot plate.



Figure 4: Experimental setup

4. This mixed nitrate solution was heated at 80°C with constant stirring until it become a gel

5.After that it is kept in oven at 120°C for 2 hours and dried. It was then crushed using mortar and pestle. Then the sample was annealed in the muffle furnace at 400°C for 2 hours



Figure 5: Oven



figure 5: annealed nickel ferrite

2.2 COPRECIPITATION METHOD

1. In coprecipitation method Nickel Nitrate Hexahydrate $[\text{Ni}(\text{NO}_3)_2] \cdot 6\text{H}_2\text{O}$, Iron Nitrate Nonahydrate $[\text{Fe}(\text{NO}_3)_3] \cdot 9\text{H}_2\text{O}$ are taken in stoichiometric amount and added in 10 ml of distilled water separately.



Figure 6: Sodium Hydrate

2. These two solutions are mixed and heated at 60°C with continuous stirring.

3. 2 M NaOH solution is added drop wise in order to keep the pH 12.

4. The precipitate is filtered out and dried in oven at 100°C .

5. crushed using mortar and pestle.

6. Annealed in the muffle furnace at 400°C for 2 hours.



Figure 7: different steps in co precipitation method

$$\text{Weight of the salt required} = \frac{\text{Molarity} \times \text{Volume} \times \text{Molecular Weight}}{1000}$$

Molecular Mass of Nickel Nitrate=290.79g

Molecular Mass of Iron Nitrate=404g

Molecular Mass of NaOH=

Weight of Nickel Nitrate=2.9079g

weight of Iron Nitrate=8.08g

weight of NaOH=8g

2.3 X-RAY DIFFRACTION (XRD)

A typical method to characterize a sample is X-ray diffraction. It can be used to ascertain the atomic structure of bigger crystals, including macromolecules and inorganic substances. It could determine specimen composition, crystal structure, and phase purity if the crystal size is too tiny. Using this method, x-ray beams are passed through it. Instead of utilising considerably greater wavelengths, which would be unaffected by the spacing between atoms, X-ray beams are chosen due to their wavelength is comparable to the spacing among atoms in the sample. This means that the angle of diffraction will be influenced by the distance of the atoms in the sample. The x-rays then go through the sample, "bouncing" off atoms in the structure to alter the trajectory of the beam at an angle different from the original beam, called theta. This is the diffraction angle. A number of these diffracted rays cancel one another out, but positive interference happens if the beams have matching wavelengths. When two x-ray beams with the same wavelength that are whole number integers combine, an additional beam with a higher amplitude is produced. This is known as constructive interference. For this particular angle of diffraction, the wave's increased amplitude results in a stronger signal. The difference between the atomic planes can then be calculated from angle of diffraction using Bragg's law.

2.3.1 BRAGG'S LAW

Laue diffraction, which establishes the angles of both coherent and incoherent scattering off a crystal lattice, is a specific example of Laue's law known as Bragg's law. An electronic cloud moves as an electromagnetic wave when X-rays strike a certain atom. Rayleigh scattering is the process by which the motion of these charges emits waves of a comparable frequency but somewhat blurred due to various factors. The connection between an x-ray light beam and the reflection from a crystal surface is essentially explained by this law.

Bragg's law states that, The X-ray's angle of incidence, and angle of scattering, are the same when it strikes a crystal surface. Additionally, constructive interference will happen when the path difference, d , is equal to n wavelengths, where n is a whole number.

$$n\lambda = 2d\sin\theta$$

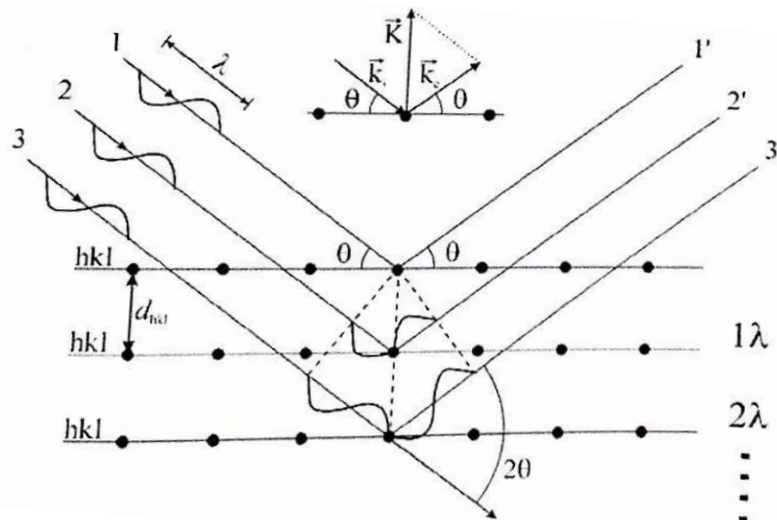


Figure 8: Bragg's Reflection from Atomic Planes

2.3.2 PARTICLE SIZE DETERMINATION FROM XRD

The outcome of X-ray diffraction exhibits the signal's strength for different diffraction angles at each of their corresponding two theta points. The resulting angle of diffraction coming from the incident x-ray beam transmitted into the samples determines the two theta positions, which correspond to a specific spacing among atoms in the samples. The number of atoms within that phase with such spacing affects the peak's strength. The quantity of crystals or molecules with those particular spacing increases with peak intensity. Peak width and crystal size have an inverse relationship. A larger crystal is associated with a thinner peak. The presence of a smaller crystal, a flaw within the structure of the crystal, or an amorphous solid, which lacks perfect crystal structure, is indicated by a wider peak. The patterns identified by XRD examination can be utilised to identify a sample's composition for smaller samples. The patterns of diffraction for compounds, elements, and minerals are stored in a huge database of these substances. When the pattern for a compound that is not known matches the position, width, and comparative altitudes of the diffraction patterns, the element's identity can be confirmed by comparing it to values from the literature and experiments.

From the XRD spectrum the particle size of nano particle is calculated using the Debye Scherrer's formula

$$D = \frac{K \times \lambda}{\beta \times \cos \theta}$$

K=constant depend on crystalline shape

$$\lambda = X \text{ ray wavelength}$$

$$\beta = FWHM$$

$$\theta = \text{diffraction angle}$$

$K=0.9$ is Scherrer's constant of the order unity for usual crystal.

2.4 SCANNING ELECTRON MICROSCOPY(SEM)

An electron microscope called a scanning electron microscope (SEM) uses a concentrated electron beam to create pictures of a sample. It gives details on the sample's surface shape and composition. The image is created by combining the position of the electron beam with the signal being detected while it is being scanned in a raster scan pattern. SEM has a far higher magnification than optical microscopes due to the electron beam's lower wavelength than that of visible light, and its resolution ranges from 1 nm to 20 nm. Due to elastic and inelastic scattering, the incident electron induces electrons to be ejected from the sample surface. Back scattered electrons are electrons with high energy which are emitted by the elastic collision of an incoming electron with the sample atom's nucleus. Back scattered electrons possess a similar energy to incident electrons. Secondary electrons are the low energy electrons released by inelastic scattering. They can be created by ejected electrons from sample atoms or by collisions with nuclei in which there is a significant energy loss. Typically, secondary electrons have an energy of 50 eV or less.

The incoming electron beam raster's pattern throughout the sample's surface to produce a SEM image. An electron detector picks up the released electrons at each location in the scanned region. On a display monitor, the brightness represents the strength of the produced electron signal. The display depicts the surface characteristics of the sample by synchronising the picture scan position to the scan of the incoming electron beam. The ratio of the image's display dimension to the samples area that the electron beam is scanning is known as the magnification of the image.

For SEM imaging, two electron detectors are typically utilised. For secondary electron imaging, scintillator detectors are utilised. A positive voltage is applied to this detector in order to draw electrons there and increase the signal-to-noise ratio. Backscattered electron detectors might be solid state or scintillator kinds. The electrons can readily go from the electron beam's source to the specimen and then to the detectors. This is because the SEM column and sampling chamber are at a reasonable vacuum. The chamber is operated at a greater vacuum for high-resolution imaging, typically between 10^{-5} and 10^{-7} Torr. Higher pressures can be used to image nonconductive, volatile, and vacuum-sensitive materials.

WORKING OF SEM

In an electron gun, the cathode emits electrons that the anode accelerates to energies between 1 and 50 keV. A series of condenser lens condense the electron beam. The scan coils' magnetic field causes the electron beam to be deflected back and forth. The electron beam scans the specimen's exterior surface in a raster pattern after having been focused using the objective lenses to a very small spot (1–5 nm). The image is created when the primary electrons interact with atomic particles on the sample surface to release secondary electrons that are then detected. It is also possible to find the electron beam's backscattered electrons. Using the backscattered electron picture, sample sections with various chemical compositions are contrasted.

ADVANTAGES

- Like a light microscope, the scanning electron microscope (SEM) employs electrons for imaging.

- Greater depth of field and far higher magnification (>100,000X) than light microscopy.
- An energy dispersive x-ray spectrometer plus scanning electron microscopy (SEM) is also used to gather both qualitative and quantitative chemical examination data.

APPLICATIONS

- The SEM is frequently employed to produce high-resolution pictures of object forms (SEI) and to demonstrate spatial changes in chemical compositions:
- Find and examine surface cracks.
- Describe the microstructures in detail.
- Examine contaminations on the surface.
- reveal differences in chemical composition throughout space.
- Make qualitative chemical analysis available.
- Crystal structures can be identified

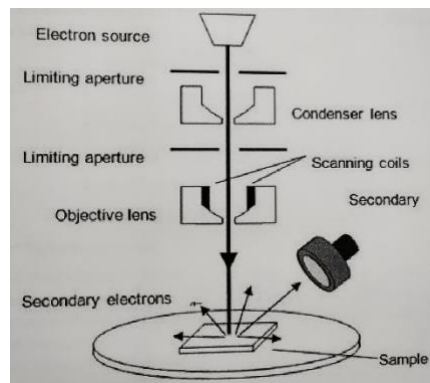


Figure 9: scanning electron microscope

2.5 UV-VISIBLE SPECTROSCOPY

The frequency of electromagnetic waves that can be captured by the objects under investigation is revealed through optical absorption. Absorption spectroscopy that operates in the ultraviolet-visible spectral band is referred to as ultra-visible

spectroscopy. This indicates that it makes use of light that falls within the visible and nearby (near UV and near infrared (NIR)) wavelength ranges. The perceived hue of the compounds involved is directly impacted by the visible spectrum absorption. Molecules go through electronic transitions in this region of the electromagnetic spectrum, and absorption detects changes from the ground state to an excited state. This may additionally be employed to determine the material's band gap. A portion of an incident light radiation that reaches a medium will pass through it, while the remaining portion of the wave will be absorbed. Electrons go from a lower

level of energy to a higher energy level as a result of photon absorption. The absorption coefficient of a material is used to gauge its capacity to absorb liquids and other substances.

The band gap and absorption coefficient can be connected using the expression if the material has a parabolic band structure.

$$\alpha = \frac{K(h - E_g)^r}{h}$$

Where E_g is the band gap, α is the absorption coefficient. The constant 'r' depends upon the nature of electronic transition. For the direct allowed transitions $r=1/2$, for indirect allowed transitions $r=3$ and for forbidden direct transitions $r=3/2$. The absorption coefficient can be deduced from the absorption or emission spectra using the relation

$$I = I_0 \exp(-\alpha x)$$

Where 'I' is the transmitted intensity, I_0 is the intensity of the incident light and 'x' is the thickness of the sample. The band gap energy can be determined by extrapolating the linear portion in the $h\nu$ versus $(\alpha h\nu)^2$. The absorption coefficient is a function of frequency.

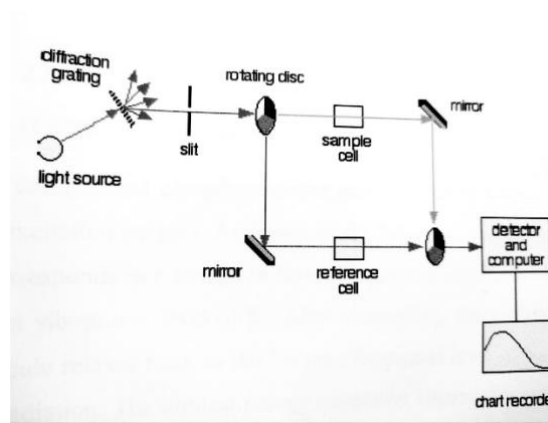


Figure 10: components of UV Visible spectrometer

2.6 PHOTOLUMINESCENCE SPECTROSCOPY

A spontaneous emission of visible light from a substance under optical excitation is known as photoluminescence (PL). A non-destructive, contactless technique for examining a material's electrical structure is photoluminescence spectroscopy. In a procedure known as photo-excitation, light is focused onto a specimen, where it gets absorbed and imparts more energy to the substance. The sample can release surplus energy by emitting light, a process known as luminescence, which is one way to do so. This luminescence is known as photoluminescence when it results from photo-excitation. The material's electrons enter allowable excited states as a result of photo-excitation. When these electrons reach their state of equilibrium states, the extra energy is either released through non-radiative processes, such as the emission of light, or through radiative processes. The variation in energy levels among the two states of electrons associated with the transition among the state of excitation and the state of equilibrium is correlated with the energy of the light that is emitted (photoluminescence). The photoluminescence's intensity and spectral composition provide a direct indicator of a number of significant material

attributes. To examine various areas and excited concentrations in the sample, the excitation energy and intensities are selected.

Monitoring the light that atoms and molecules release after absorbing photons is the focus of PL spectroscopy. Materials that show photoluminescence can use it. Inorganic as well as organic substances of almost any size can be characterised using PL spectroscopy, and the specimens can be in a gaseous, liquid, or solid form. In PL spectroscopy, electromagnetic radiation within the Ultraviolet and visible bands is used. Four factors: intensity, emission wavelength, emission peak bandwidth, and emission stability—are used to describe the sample's PL emission characteristics. A material's PL characteristics may alter in various environmental conditions or when additional molecules are present.

Additionally, the PL emission characteristics can alter as dimensions are shrunk to the nanoscale; in particular, a size-dependent shift in the wavelength of emission can be seen. Additionally, PL spectroscopy can be used to investigate material characteristics including band gap, recombination mechanisms, and degree of impurity because the released photon matches to the difference in energy between the states. Numerous material properties can be characterised using photoluminescence (PL) studies. Knowledge on the level of quality of surface and interfaces can be derived from the PL signal's strength.

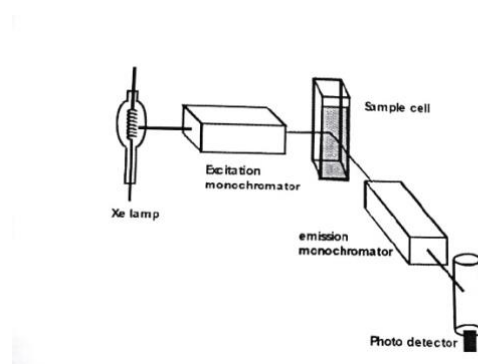


Figure 11: photoluminescence spectrometer

The activation of the material's electronic system and the resulting emission of photons are at least two processes in the process of luminescence. Photons are captured and electronic excitations are produced when light with a high enough energy is incident on a substance. These excitations eventually subside, and the electrons go back to their ground state. The light that is released is known as PL if radiative relaxation takes place. It is possible to gather and analyse this light to learn a multitude of details about the photoexcited substance. non radiative as well as radiative Recombination rates are measured by the PL intensity. Figure displays a schematic block diagram of the photoluminescence setup's parts. a wavelength band is chosen by an excitation monochromator. The sample receives this monochromatic light, which produces luminescence emission. The second emission monochromator, which chooses a band of the wavelengths and illuminates them onto the photon counting detector, receives the emitted light. The host computer and system controller receive a signal from the detector, which is then used to alter and display the data using specialised software.

CHAPTER 3

RESULTS AND DISCUSSIONS

3.1 STRUCTURAL CHARACTERIZATION

In this work, structural characterization is done using X-ray diffraction method. The XRD pattern of Nickel Ferrite nanoparticles is studied with $\text{Cu-K}\alpha$ radiation (wavelength=1.5406 \AA) in the range of $2\theta = 10^\circ$ to 80° . The crystallite size of nickel ferrite nanoparticles are investigated using Scherrer's equation.

$$D = \frac{k \times \lambda}{\beta \times \cos\theta}$$

Where D is the particle size, k a fixed number which is 0.9, λ the X-ray wavelength, θ the Bragg's angle in degree, and β the full width at half maximum of the peak in radians.

For a particular sample, particle size for 2θ values corresponding to the prominent diffraction peaks are calculated and average particle size is determined. The same procedure is done for other prepared samples.

a) X-RAY diffraction analysis of Nickel Ferrite nanoparticles prepared by Sol Gel method

The powder x ray pattern of nickel ferrite is shown in the figure below. The sample shows diffraction peaks corresponding to reflection planes (111), (220), (311), (222), (400), (422), (511), (440), (620), (533) at 2θ values 18.446, 30.288, 35.687, 37.262, 43.315, 53.827, 57.447, 62.969, 71.681, 74.688 degrees respectively. On comparing with the standard database (JCPDS card No.10-0325), the values of prepared nickel ferrite nanoparticles are found to be fairly in good agreement, thus confirming the cubic spinel structure of Nickel ferrite. In the x ray pattern, no extra peaks were detected.

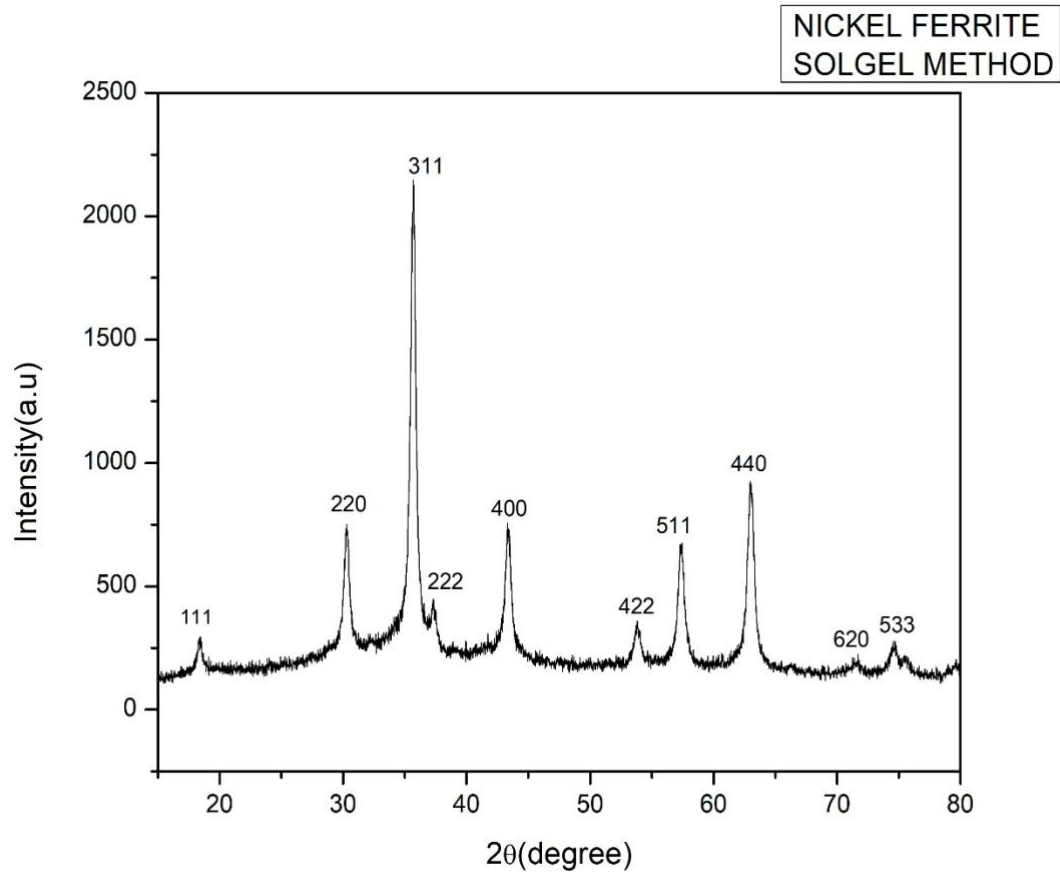


Figure.1.XRD pattern of Nickel ferrite prepared by Sol Gel method.

PARTICLE SIZE DETERMINATION

Using the XRD data in Debye-Scherrer formulae the particle size of nickel ferrite nanoparticles is calculated as,

For $2\theta = 18.446^\circ$

$$\beta = 0.015095 \text{ A}^\circ$$

$$\text{Particle size, } D = \frac{K \times \lambda}{\beta \times \cos\theta}$$

$$D = \frac{0.9 \times (1.5 \times 10^{-10})}{0.015095 \times \cos(18.446^\circ)}$$

$$= 9.06049 \text{ nm}$$

2θ (degree)	θ (degree)	θ (radian)	FWHM (degree)	FWHM (radian)	PARTICLE SIZE(nm)
18.446	9.223	0.160972	0.86488	0.015095	9.06049
30.288	15.144	0.264313	0.69069	0.012055	11.6017
35.687	17.8435	0.311428	0.55698	0.009721	14.589
37.262	18.631	0.325172	1.05522	0.018417	7.73553
43.315	21.6575	0.377995	0.74736	0.013044	11.1358
53.827	26.9135	0.469729	0.96457	0.016835	8.99308
57.447	28.7235	0.50132	0.73962	0.012909	11.9254
62.969	31.4845	0.549508	0.71956	0.012559	12.6053
71.681	35.8405	0.625535	1.65409	0.028869	5.76851
74.688	37.344	0.651776	1.77944	0.031057	5.46766

Hence average particle size is $D = 9.88825 \text{ nm}$

LATTICE PARAMETER

$$\text{lattice parameter} = d \times \sqrt{(h^2 + k^2 + l^2)}$$

$$= (2.44 \times 10^{-10}) \times \sqrt{(1^2 + 1^2 + 1^2)}$$

$$= 8.1210 \text{ \AA}$$

$$\text{cell volume} = a^3$$

$$= (8.1210)^3$$

$$= 534.648 \text{ \AA}^3$$

2 theta	d	a
35.67281	2.44858E-10	8.12101E-10
18.446	4.67939E-10	8.10493E-10
30.288	2.87086E-10	8.12002E-10
35.687	2.44764E-10	8.11789E-10
37.262	2.34762E-10	8.13241E-10
43.315	2.0322E-10	8.12882E-10
53.827	1.65693E-10	8.11726E-10
57.447	1.5606E-10	8.10914E-10
62.969	1.43604E-10	8.1235E-10
71.681	1.28089E-10	8.10105E-10
74.688	1.2364E-10	8.10763E-10

b) X-RAY DIFFRACTION ANALYSIS OF NICKEL FERRITE NANOPARTICLES PREPARED BY CO-PRECIPIATION METHOD

The prepared Nickel Ferrite nanoparticles using co-precipitation method are characterized using XRD technique and the resultant XRD pattern is obtained.

The sample shows diffraction peaks corresponding to reflection planes (111), (220), (311), (222), (400), (422), (511), (440), (620), at values 18.56771, 30.45162, 35.84511, 35.9292, 43.55707, 54.00613, 57.52822, 63.15114, 69.37475 degrees respectively. On comparing with the standard database (JCPDS card No. 10-0325), the values of prepared nickel ferrite nanoparticles are found to be fairly in good agreement, thus confirming the cubic spinel crystal structure. The XRD pattern of Nickel ferrite nanoparticles prepared by co-precipitation method is shown below

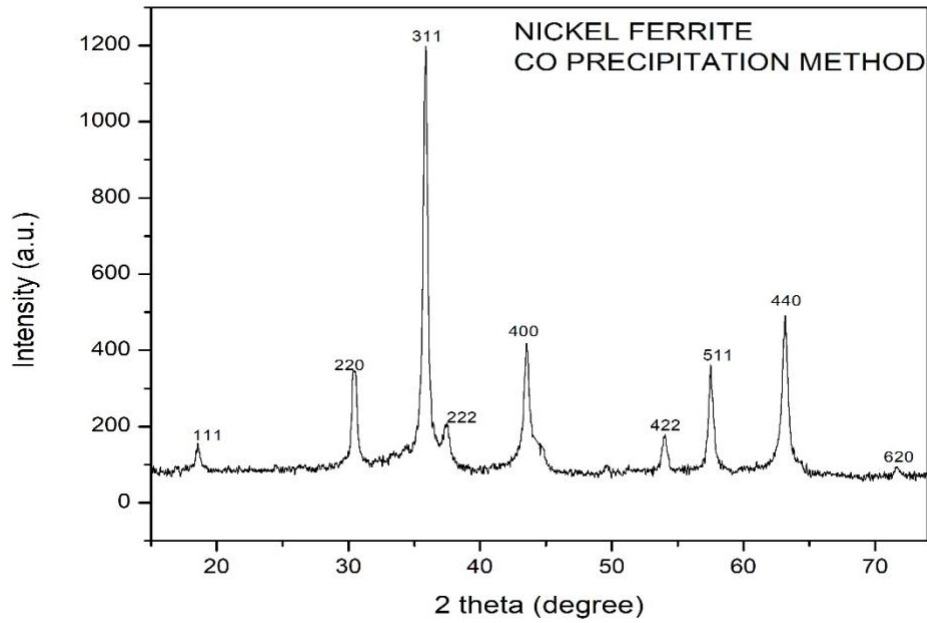


Figure.2. XRD pattern of Nickel Ferrite by co precipitation method.

- PARTICLE SIZE DETERMINATION

Using the XRD data in Debye-Scherrer formulae the particle size of nickel ferrite nanoparticles is calculated as,

For $2\theta = 18.56771$

$$\beta = 0.008382$$

$$\text{Particle size, } D = \frac{K \times \lambda}{\beta \times \cos \theta}$$

$$D = \frac{0.9 \times (1.5 \times 10^{-10})}{0.008382 \times \cos(18.5677^\circ)}$$

$$= 16.3202 \text{ nm}$$

2θ (degree)	θ (degree)	θ (radian)	FWHM (degree)	FWHM (radian)	Particle size (m)
18.56771	9.283855	0.162034	0.48024	0.008382	1.63202E-08
30.45162	15.22581	0.265741	0.5153	0.008994	1.55566E-08
35.84511	17.92256	0.312808	0.38911	0.006791	2.08924E-08
35.9292	17.9646	0.313541	3.63569	0.063455	2.23654E-09
43.55707	21.77854	0.380107	0.83047	0.014494	1.00298E-08
54.00613	27.00307	0.471292	0.48541	0.008472	1.78846E-08
57.52822	28.76411	0.502028	0.51118	0.008922	1.72614E-08
63.15114	31.57557	0.551098	0.62418	0.010894	1.45456E-08
69.37475	34.68738	0.605409	4.96894	0.086724	1.89312E-09

Average particle size, $D = 12.9578$ nm

- Lattice parameter

$$\text{lattice parameter} = d \times \sqrt{(h^2 + k^2 + l^2)}$$

$$\begin{aligned} \text{lattice parameter} &= (4.64898 \times 10^{-10}) \times \sqrt{(1^2 + 1^2 + 1^2)} \\ &= 1.54189 \text{ \AA} \end{aligned}$$

$$\text{Average lattice parameter} = 7.94074 \times 10^{-10} \text{ \AA}$$

2θ	d	a
18.56771	4.64898E-10	1.54189E-09
30.45162	2.8558E-10	4.94638E-10
35.84511	2.43719E-10	6.89342E-10
35.9292	2.43168E-10	8.06495E-10
43.55707	2.02145E-10	7.00252E-10
54.00613	1.65184E-10	6.60737E-10
57.52822	1.55859E-10	7.63549E-10
63.15114	1.43233E-10	7.4426E-10
69.37475	1.31787E-10	7.45502E-10

- CELL VOLUME

$$\text{Cell volume} = a^3$$

$$= (7.94074)^3$$

$$= 500.7 \text{ \AA}^3$$

Table 1.XRD parameters of Nickel ferrite Nanoparticles

Chemical Formulae	$NiFe_2O_4$	$NiFe_2O_4$
Method of Preparation	SOL GEL	CO PRECIPITATION
Lattice Constant 'a'	8.1210 \AA	7.94074 \AA
Average Particle size 'D'	9.06049 nm	$12.9578 \times 10^{-9} \text{ m}$
Cell Volume	534.648 \AA^3	500.7 \AA^3

3.2 MORPHOLOGICAL ANALYSIS

We use scanning electron microscopy (SEM) to analyse the morphological characteristics of nickel ferrite nanoparticles. The figures show irregular structures. They are highly crystallized particles which are agglomerated. The formation of agglomerates could be due to magnetic attraction.

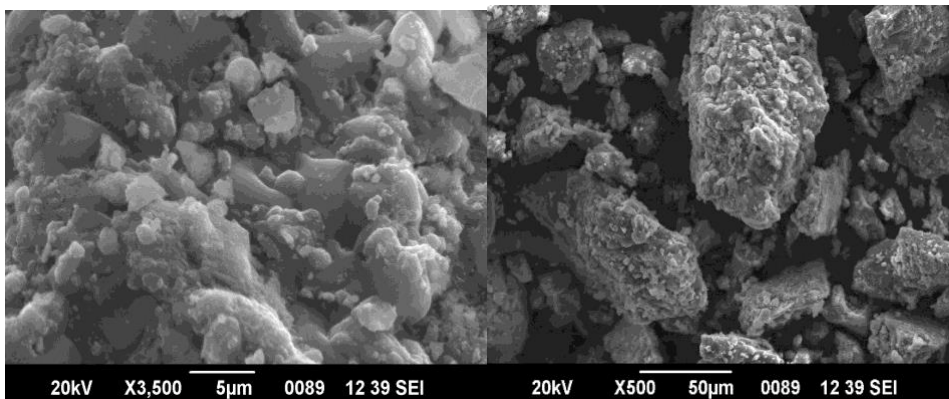


Figure 3: Sem images of sample prepared by co precipitation method

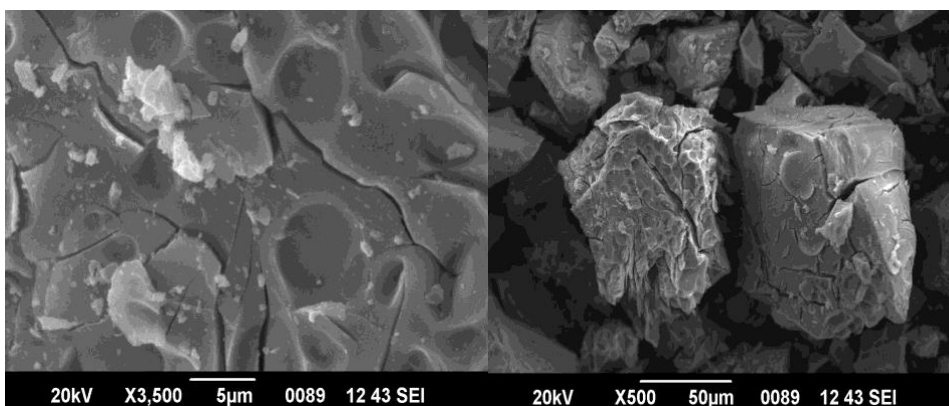


figure 4: Sem images of Nickel Ferrite nanoparticles prepared by solgel method

3.3 OPTICAL CHARACTERIZATION

In this work optical characterization is done using UV visible absorption and photoluminescence. The prepared samples are studied using UV- visible and PL spectra.

3.3.1 UV-VISIBLE ABSORPTION OF NICKEL FERRITE NANOPARTICLES

The UV-Visible absorption spectra of nickel ferrite nanoparticles prepared by solgel method is shown below. The characteristic peaks appear in the wavelength range 200 –800 nm and the peak position reflects the band gap of the nanoparticles.

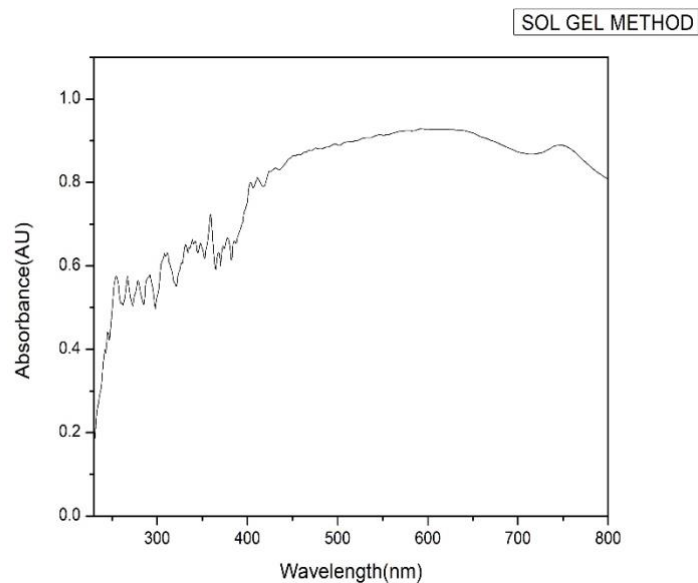


Figure 5: uv visible absorption spectra of nickel ferrite prepared by solgel method

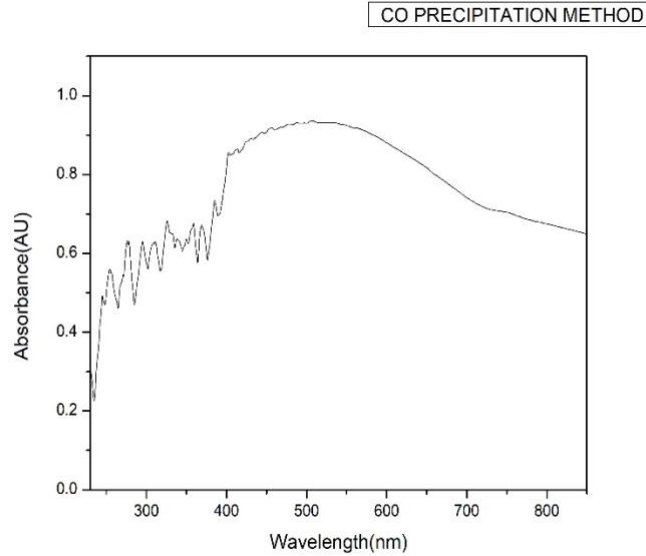


Figure 6: uv-visible absorption spectra of nickel ferrite prepared by co precipitation method

The strongest absorption peak appears at 404 nm for solgel method and at 402nm for co precipitation method. The fundamental absorption, which corresponds to electron excitation from the valence band to conduction band, can be used to determine the value of optical band gap of the synthesized nickel ferrite nanoparticles.

Band gap energy can be calculated by the formula

$$Eg = \frac{hc}{\lambda}$$

Here h is the Planck's constant, λ is the wavelength of absorption.

- **BANDGAP ENERGY DETERMINATION**

From the optical absorption data, a graph is plotted with $h\nu$ versus $(\alpha h\nu)^2$ to determine the bandgap energy for the sample. By extrapolating the linear portion of the curve to meet $h\nu = 0$, one can calculate the bandgap energy in eV. The Figure shows the $h\nu$ versus $(\alpha h\nu)^2$ graph of nickel ferrite nanoparticles prepared by solgel method.

The band gap energy was calculated using Tauc's plot. According to Tauc's equation for a direct bandgap material the absorption coefficient near the band edge is:

$$\alpha = \frac{A}{h\nu} (h\nu - E_g)^{\frac{1}{2}}$$

where α is the absorption coefficient, $h\nu$ the photon energy, E_g the band gap energy, and A is a constant depending on the type of transition. Above equation can be rearranged and written in the form:

$$(\alpha h\nu)^2 = A^2 (h\nu - E_g)$$

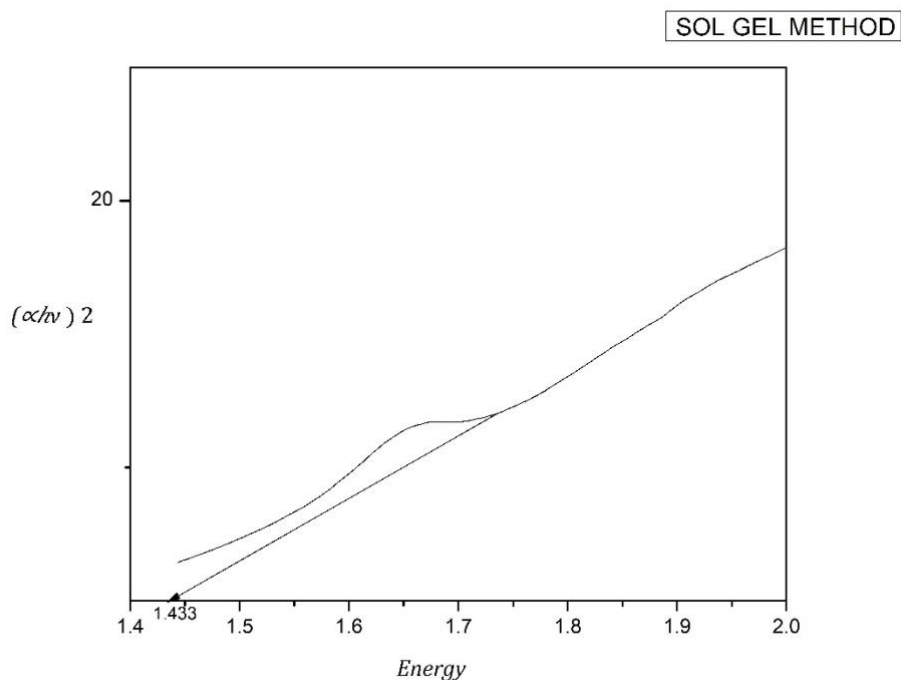


Figure7: Tauc plot determining the indirect band gap of nickel ferrite nanoparticles prepared by solgel method

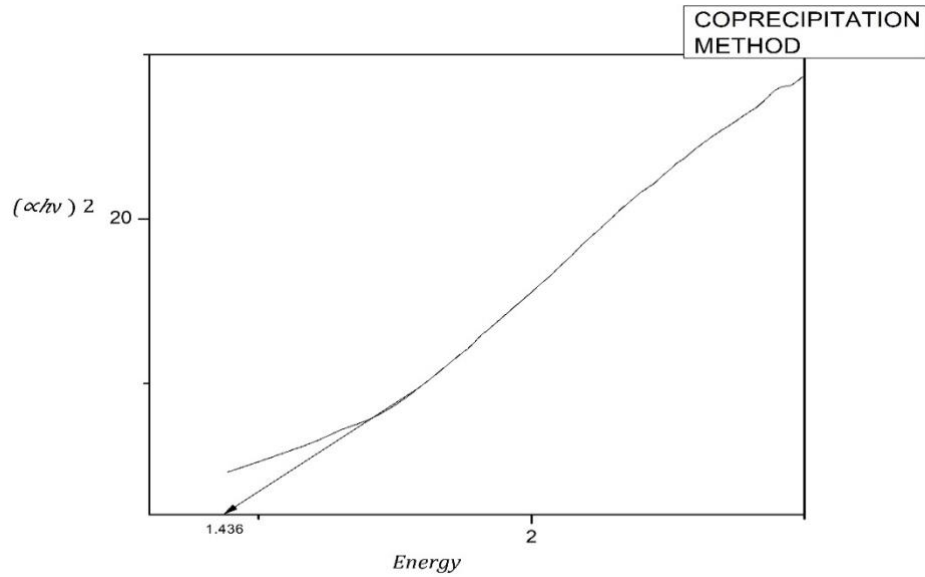


Figure8: Tauc plot determining the indirect band gap of nickel ferrite nanoparticles prepared by coprecipitation method

band gap is an important parameter that determines the electrical conductivity of the materials. Band gap is the amount of energy required to promote a valence electron from valence band to conduction band and the electron is free to move within the crystal lattice and serve as a charge carrier to conduct electric current. Hence, the energy band gap of the ferrite nanoparticles are important for allowing devices to operate at higher temperatures under normal conditions. This property makes them highly attractive for military applications.

The band gap of Nickel Ferrite is about 1.53 whereas band gap energy of nickel ferrite nanoparticles that we obtained was ~1.43 eV (1.433 eV by solgel method and 1.436 eV by coprecipitation method). It was observed that band gap energy is approximately same for both the methods. We obtained the lowest value of band gap energy(1.43eV) i.e., narrower the band gap energy, higher the photocatalytic activity.

3.3.2 PHOTOLUMINESCENCE (PL) STUDIES OF NICKEL FERRITE NANOPARTICLES PREPARED BY SOLGEL AND CO PRECIPITATION METHOD

Photoluminescence emission spectrum of nickel ferrite nanoparticles at an excitation wavelength of 239 nm are recorded. And the PL spectra revealed two emission peaks one in the uv region centred around 385 nm and other in the visible region around 523 nm for both solgel and co precipitation method. UV emission also known as near band edge emission (NBE) results from the transformation of electrons between their shallow levels which are located near their related band edges i.e valence band for acceptors and conduction band for donors. Visible emission that often referred to as deep level emission (DPE) originates due to transitions from deep donor levels to the valence band.

Sharp peaks in the spectra are attributed to the exchange of charges between Fe^{3+} and the surrounding O^{2-} ions at octahedral sites. The peak at 523 nm recombination of photo-generated holes with ionized charge species from oxygen vacancies and the nickel interstitials. Emission at 385 nm is due to the transition from $\text{Ni}^{2+} (t_{2g}) \rightarrow \text{Fe}^{3+} (t_{2g})$.

PL spectrum is often mistaken for absorption spectrum. However, absorption spectrum measures transitions from the ground to the excited electron state and PL concerns with vice versa transitions—from the excited to the ground state. An excitation spectrum is very much alike to absorption spectrum, as it is represented as intensity versus excitation wavelength. The wavelength at which the molecule is absorbing energy can be equal to the excitation wavelength.

The prepared sample showed luminescence peaks in visible region. Hence the prepared materials may be useful in light absorption, photocatalytic degradation, magneto-optical devices and some others and it also showed emission peak in the uv region which is applicable to the water quality detection.

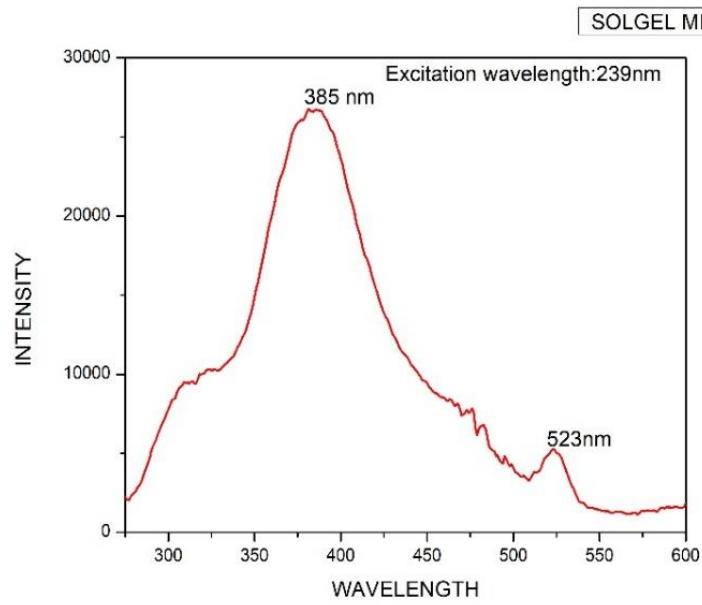


Figure 9: PL emission spectra of nickel ferrite prepared by sol-gel method

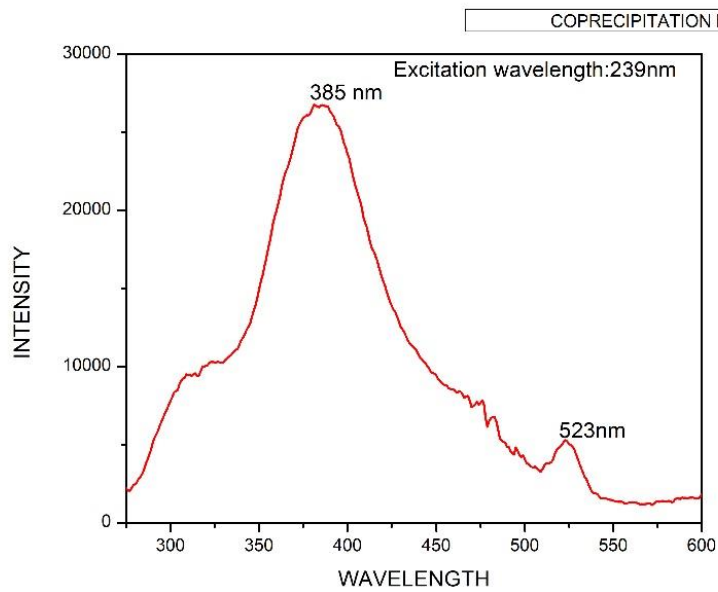


Figure 10: PL emission spectra nickel ferrite nanoparticles prepared by co-precipitation method

3.4 CONCLUSION

Nickel ferrite nanoparticles are successfully prepared by solgel and coprecipitation method. X ray diffraction confirms the cubic spinel phase of nickel ferrite with an average crystal size of 9.06049 nm from solgel method and 12.9578nm from coprecipitation method. Sem confirms highly crystallized agglomerated irregular morphology for nickel ferrite nanoparticles prepared from both methods. Nickel ferrite prepared from solgel method and co precipitation method show maximum absorption at 404 nm and at 402 nm respectively. And the band gap energies are found to be 1.433 and 1.436 ev. PL spectra revealed two emission peaks one in the uv region centred around 385 nm and other in the visible region around 523 nm which are due to the near band edge emission and deep level emissions respectively. Since Nickel ferrite has emissions in the UV, Visible and near infra-red regions it can be used in cell imaging. Also, Nickel Ferrite nanoparticles have inherent multicolour photoluminescence. Nickel ferrite nanoparticles can adhere to osteosarcoma cells and produce light under illumination with appropriate wavelength and intensity. Also, since it shows emissions all the way from uv to near infrared region it can act as a sensor. a sensor based on pure NiFe_2O_4 nanomaterial showed selective response towards LPG at 400°C with a response time of few seconds and good reproducibility.

3.5 FUTURE SCOPE

The production of ferrites will continue to increase each year, even in the future, as will the advancement of electronic technologies. If researchers and engineers who are concerned with ferrites take a deeper look at the future aspects of ferrites and devote themselves to the subjects of great value, the future of ferrites will experience a steady and more advanced prosperity in science and technology, and their industries will be continue to grow in the future.

Nickel ferrite nanoparticles have inherent multicolour photoluminescence. Therefore, it can be used in cell imaging. Nickel ferrite nanoparticles can adhere to osteosarcoma cells and produce light under illumination with appropriate wavelength and intensity.

3.6 REFERENCES

1. Azizurrahman Ansari, Vishal Kumar Chakradhary, M.J. Akhtar, Synthesis of nickel ferrite nanoparticles via chemical co-precipitation method, Indian Institute of Technology, Kanpur, Uttar Pradesh, 208016, India.
2. R. Kesavamoorthi, A.N. Vigneshwaran, Vijayalakshmi Sanyal and C. Ramachandra Raja*, Synthesis and characterization of nickel ferrite nanoparticles by sol - gel auto combustion method, Department of Physics, Government Arts College (Autonomous), Kumbakonam - 612 001.
3. Walmir E. Pottker, Rodrigo Ono, Miguel Angel Cobos, Antonio Hernando, Jefferson F.D.F. Araujo, Antonio C.O. Bruno, Sidney A. Lourenço, Elson Longo, Felipe A. La Porta, Influence of order-disorder effects on the magnetic and optical properties of $NiFe_2O_4$ nanoparticles, Department of Physics, Pontificia Universidade Catolica do Rio de Janeiro, Rio de Janeiro 22451-900, Brazil.
4. R.C. Rai · S. Wilser · M. Guminiak · B. Cai · M.L. Nakarmi, Optical and electronic properties of Nickel ferrite and Cobalt ferrite thin films, Department of Physics, SUNY College at Buffalo, Buffalo, NY 14222, USA.
5. Seema Joshi , Manoj Kumar, Sandeep Chhoker , Geetika Srivastava , Mukesh Jewariya , V.N. Singh, Structural, magnetic, dielectric and optical properties of nickel ferrite nanoparticles synthesized by co-precipitation method, Department of Physics and Materials Science and Engineering, Jaypee Institute of Information Technology, Noida 201307, India.
6. M. Hjiri, N. H. Alonizan, M. M. Althubayti, S. Alshammari, H. Besbes, M. S. Aida Preparation and photoluminescence of Nickel ferrite nanoparticles, Department of Physics, Faculty of Sciences, King Abdulaziz University, 21589 Jeddah, Saudi Arabia.

7. P. Paramasivan, P. Venkatesh, A Novel Approach: Hydrothermal Method of Fine Stabilized Superparamagnetics of Cobalt Ferrite Nanoparticles, Department of Chemistry, Pachaiyappa's College, Chennai-30, India.

8. W. F. J. Fontijn, P. J. van der Zaag, L. F. Feiner, R. Metselaar, M. A. C. Devillers, A consistent interpretation of the magneto-optical spectra of spinel type ferrites(invited), Department of Solid State Chemistry and Materials Science, Eindhoven University of Technology, P.O. Box 513, 5600 MB Eindhoven, The Netherlands.

9.L. Renuka , Preeti Mishra, Y.S. Vidya , G. Banuprakash, K.S. Anantharaju, K. N. Harish, Facile surface modification of Nickel ferrite nanomaterial by different routes: Photoluminescence and photocatalytic activities, Department of Chemistry, Rajalakshmi Engineering College, Thandalam, Chennai 602105, India.

10.Nishant Kumar,Rakesh K r Singh, Influence of Li^{+} (alkali metal) ion on structural, optical and magnetic properties of nickel ferrite nanomaterials for multifunctional applications, Aryabhata Center for Nanoscience and Technology, Aryabhata Knowledge University, Patna Pin-800001, India.

11. Souvanik Talukdar, Rupali Rakshit, Andre Kr ¨ amer, Frank A. Muller and Kalyan Mandala, Facile surface modification of nickel ferrite nanoparticles for inherent multiple fluorescence and catalytic activities, Department of Condensed Matter Physics & Material Science, S. N. Bose National Centre for Basic Sciences, JD Block, Sector-III, Salt Lake, Kolkata-700106, India.

12. T.R. Mehdiyev, A.M. Hashimov ,Sh.N. Aliyeva, I.F. Yusibova, A.V. Agashkov ,B.A. Bushuk, luminescent and optical properties of (ni, zn) ferrites,

Institute of Physics, Azerbaijan National Academy of Sciences, Baku,
Azerbaijan.

13. Binu P Jacob, Ashok Kumar, R P Pant, Sukhvir Singh, E M Mohammed, Influence of preparation method on structural and magnetic properties of nickel ferrite nanoparticles, Department of Physics, Maharaja's College, Ernakulam 681 011, India.

14. R. Galindo, N. Menendez, P. Crespo, V. Velasco, O. Bomati-Miguel, D. Díaz-Fernández, P. Herrasti, Comparison of different methodologies for obtaining nickel nanoferrites, c Departamento de Física Aplicada and Instituto Nicolás Cabrera, Facultad de Ciencias Universidad Autónoma de Madrid, Cantoblanco, E-28049 Madrid, Spain.

15. M. Madhukara Naik, H.S. Bhojya Naik, G. Nagaraju, M. Vinuth, K. Vinu, S.K. Rashmi, Effect of aluminium doping on structural, optical, photocatalytic and antibacterial activity on nickel ferrite nanoparticles by sol-gel auto-combustion method, Department of studies and research in industrial chemistry, School of chemical sciences, Kuvempu University, Shankaraghatta, Karnataka 577451, India.

16. K. S. Ashraf Ali, V. Mohanavel, C. Gnanavel, V. Vijayan, N. Senthilkumar, Structural and optical behavior of SnS₂/NiFe₂O₄ NCs prepared via novel two-step synthesis approach for MB and RhB dye degradation under sun light irradiation, Department of Mechanical Engineering, C. Abdul Hakeem College of Engineering & Technology, Melvishram, Vellore 632509, Tamil Nadu, India.

17. M. Madhukara Naika, M. Vinuthb, V. Udaya Kumara, K.H. Hemakumarc, G. Preethia , M. Prathap Kumara, G. Nagaraju, A Facile Green Synthesis of Nickel Ferrite Nanoparticles using Tamarindus Indica Seeds for Magnetic and Photocatalytic Studies, Department of Chemistry, MVJ College of Engineering, Bengaluru 560 067 Karnataka, India.

18. Masaki Kobayashi, Munetoshi Seki, Masahiro Suzuki, Miho Kitamura, Koji Horiba, Hiroshi Kumigashira, Atsushi Fujimori, Masaaki Tanaka, and Hitoshi Tabata, Inter-valence charge transfer and charge transport in the spinel ferrite ferromagnetic semiconductor Ru-doped Cobalt Ferrite, Department of Physics, The University of Tokyo, 7-3-1 Hongo, Bunkyo-ku, Tokyo 113-0033, Japan.

19. Kwang Joo Kim, Han Seung Lee, Myoung Hee Lee, and Sung Ho Lee, Comparative magneto-optical investigation of d–d charge–transfer transitions in Fe_3O_4 , CoFe_2O_4 , and NiFe_2O_4 , Department of Physics, Konkuk University, Seoul 143-701, Korea.

20. Suresh Sagadevan, Zaira Zaman Chowdhury, Rahman F. Raque, Preparation and Characterization of Nickel Ferrite nanoparticles via co-precipitation method, Nanotechnology & Catalysis Research Centre, University of Malaya, Kuala Lumpur 50603, Malaysia.

